

Metabolic flux analysis for a *ppc* mutant *Escherichia coli* based on ¹³C-labelling experiments together with enzyme activity assays and intracellular metabolite measurements

Lifeng Peng^a, Marcos J. Arauzo-Bravo^a, Kazuyuki Shimizu^{a,b,*}

^a Department of Biochemical Engineering and Science, Kyushu Institute of Technology, Iizuka, Fukuoka 820-8502, Japan

^b Institute for Advanced Bioscience, Keio University, Tsuruoka, 997-001 Yamagata, Japan

Received 28 January 2004; received in revised form 12 March 2004; accepted 5 April 2004

First published online 16 April 2004

Abstract

The physiology and central metabolism of a *ppc* mutant *Escherichia coli* were investigated based on the metabolic flux distribution obtained by ¹³C-labelling experiments using gas chromatography–mass spectrometry (GC–MS) and 2-dimensional nuclear magnetic resonance (2D NMR) strategies together with enzyme activity assays and intracellular metabolite concentration measurements. Compared to the wild type, its *ppc* mutant excreted little acetate and produced less carbon dioxide at the expense of a slower growth rate and a lower glucose uptake rate. Consequently, an improvement of the biomass yield on glucose was observed in the *ppc* mutant. Enzyme activity measurements revealed that isocitrate lyase activity increased by more than 3-fold in the *ppc* mutant. Some TCA cycle enzymes such as citrate synthase, aconitase and malate dehydrogenase were also upregulated, but enzymes of glycolysis and the pentose phosphate pathway were downregulated. The intracellular intermediates in the glycolysis and the pentose phosphate pathway, therefore, accumulated, while acetyl coenzyme A and oxaloacetate concentrations decreased in the *ppc* mutant. The intracellular metabolic flux analysis uncovered that deletion of *ppc* resulted in the appearance of the glyoxylate shunt, with 18.9% of the carbon flux being channeled via the glyoxylate shunt. However, the flux of the pentose phosphate pathway significantly decreased in the *ppc* mutant.

© 2004 Federation of European Microbiological Societies. Published by Elsevier B.V. All rights reserved.

Keywords: *ppc* mutant *Escherichia coli*; 2-Dimensional nuclear magnetic resonance; Gas chromatography-mass spectrometry; Metabolic flux analysis

1. Introduction

In *Escherichia coli*, glycolysis, the pentose phosphate pathway and the tricarboxylic acid (TCA) cycle play important roles in providing precursor compounds, energy and reducing power for other pathways. Manipulation of these central pathways by genetic and/or environmental modifications is of significant interest from both the fundamental science and the applied biotechnology points of view [1,2]. While some single-gene-knockout mutants in central metabolism preclude

growth on glucose, the majority may potentially be compensated for either by using alternative enzymes or by rerouting carbon flux through alternative pathways. The quantitative description of metabolic and physiological responses to an individual gene knockout can provide insights into the control and regulation of central metabolism.

Among the central metabolic pathway enzymes of *E. coli*, PEP carboxylase (Ppc) plays an anaplerotic role in replenishing oxaloacetate consumed in biosynthetic reactions and keeping the TCA cycle intermediates from starvation. Chang et al. [3] reported increased D-lactate production by a *ppc* mutant of *E. coli* under anaerobic condition. Farmer and Liao [4] overexpressed Ppc and/or induced glyoxylate shunt by *fadR* to elevate the TCA

* Corresponding author. Tel.: +81-948-29-7817; fax: +81-948-29-7801.

E-mail address: shimi@bse.kyutech.ac.jp (K. Shimizu).

cycle activity for the reduction of acetate excretion under aerobic conditions, since acetate excretion is a major obstacle in enhancing the recombinant protein production. However, little has been investigated about the effect of the *ppc* knockout on the metabolism of *E. coli* under aerobic condition so far.

In the present study, we report the effects of an *E. coli* *ppc* mutation based on ^{13}C -labelling experiments followed by the measurements of the isotopomer distributions of the proteinogenic amino acids using gas chromatography–mass spectrometry (GC–MS) and 2-dimensional nuclear magnetic resonance (2D NMR) together with the measurements of enzyme activities and intracellular metabolite concentrations.

2. Materials and methods

2.1. Bacterial strains and culture conditions

Escherichia coli BW25113 (*lacI^q rrnB_{T14} ΔlacZ_{WJ16} hsdR514 ΔaraBAD_{AH33} rhaBAD_{LD78}*) and its *ppc* mutant strain JWK3928 were used in the present study. The mutant was constructed by deleting the *ppc* gene using a one-step method [5].

Strains were grown in M9 minimal medium as described previously [6] with the exception that the glucose concentrations: 5 g l⁻¹ for batch cultivation and 4 g l⁻¹ for chemostat culture. All batch and chemostat cultivations were conducted at 37 °C in a 1 liter fermentor with pH controlled at 7.0. The airflow was maintained at 0.5 min⁻¹ and the dissolved oxygen kept above 30% of air saturation all the time. The medium was fed into the fermentor at a dilution rate (*D*) of 0.2 h⁻¹ during chemostat growth.

Labeling experiments were initiated after the chemostat culture had reached a steady state, which was inferred by the stable oxygen and carbon dioxide concentrations in the off-gas and constant optical density in the effluent for at least two residence times, and then the feeding medium was replaced by a medium containing the mixture of 0.4 g of uniformly labeled glucose [U- ^{13}C], 0.4 g of first-carbon-labeled glucose [1- ^{13}C] and 3.2 g of naturally labeled glucose per liter. Biomass samples for GC–MS and 2D NMR analysis were taken in two volume exchanges, so that 86% of the biomass was ^{13}C -labelled according to the first-order wash-out kinetics.

2.2. Analytical procedures

Dry cell weight (DCW) was monitored by optical density (OD₆₀₀) and calculated from previously determined OD₆₀₀-to-DCW correlations. Glucose concentration and acetic acid concentration were measured with enzymatic kits (Wako Co., Osaka, Japan; Roche Molecular Biochemicals, Mannheim, Germany). Oxy-

gen and carbon dioxide concentrations in the off-gas of the bioreactor were monitored by a gas analyzer (Model LX-750, Iijima Electronics MFG. Co., Japan).

Preparation of cell-free extracts and assay procedures for enzyme activities were described previously [7]. Each enzyme was measured three times for the same culture.

Intracellular metabolite concentrations in quenched cell broth were measured by enzymatic procedures using a fluorescence spectrophotometer (F-4010, Hitachi Co., Japan) as described by Schaefer et al. [8] and Bergmeyer [9]. Each metabolite was determined in triplicate for the same culture.

Preparation of cellular amino acids for 2D NMR measurement was previously described by Yang et al. [10]. 2D proton-detected heteronuclear ^1H , ^{13}C multiple-quantum correlated nuclear magnetic resonance (2D HMQC NMR) spectra were recorded on a Bruker Avance 400 spectrometer (Bruker, Karlsruhe, Germany). The assignment of carbon signals and the spectra processing were performed according to the protocol of Schmidt et al. [11]. Bruker XWINNMR program was used to quantify the relative abundances of singlet, doublet, and doublet of doublets signals to the overall multiplet patterns.

Preparation of biomass hydrolysates and recording of GC–MS spectra were carried out according to Zhao and Shimizu [6]. The analysis was performed using Auto-System XL GC (Perkin–Elmer Co., USA) equipped with a DB-5MS column (30 m × 0.25 mm × 0.25 μl, Agilent Co., USA), which was connected to a TurboMass Gold mass spectrometer (Perkin–Elmer Co., USA). The peak assignment and MS data processing were made by Turbomass Gold program (Perkin–Elmer Co., USA). Skewing effects of natural isotopes (^2H , ^{13}C , ^{17}O , ^{18}O , ^{15}N , ^{29}Si , ^{30}Si) were corrected using the algorithm proposed by Paul Lee [12].

2.3. Metabolic flux calculation

The bioreaction network was constructed based on the literature [1,2,13,14] as well as the enzyme activity analysis in the present study. The glyoxylate shunt was not considered in the wild type since this pathway is normally repressed during growth with glucose [13]. The resulting network consisted of 21 reactions with 19 metabolites, giving a stoichiometric matrix with a rank of 19 (see Appendix A). The net free fluxes taken into account were 6-phosphogluconate dehydrogenase (6PGDH) and citrate synthase (CS) that were chosen as the net free fluxes, and 10 exchange fluxes considered were (Pgi, Eno, Rpi, Rpe, Tkt1, Tkt2, Tal, ICDH, Mdh, Ppc/Pck: (see the legend to Fig. 1 and Appendices A and B for further definitions). Additionally, the glyoxylate shunt was included in the network of the *ppc* mutant since it was demonstrated to be activated as an alternative anaplerotic pathway upon *ppc* mutation by the

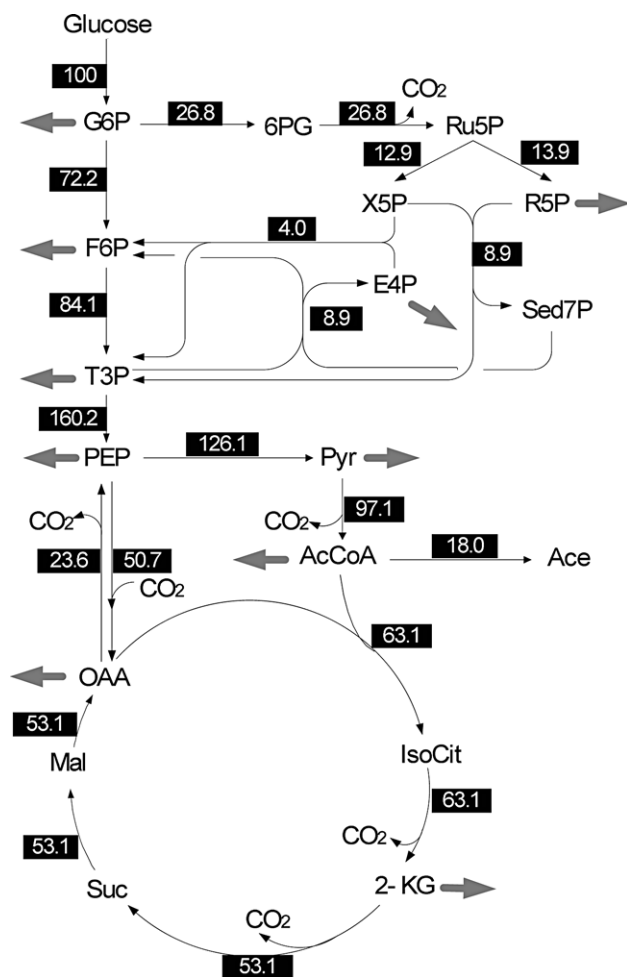


Fig. 1. Metabolic flux distribution in the chemostat culture of the wild type *E. coli*. Numbers in the black box represent the estimated net fluxes at a dilution rate of 0.2 h^{-1} . Flux values are given in parentheses in $\text{mmol g}_{\text{DCW}}^{-1} \text{ h}^{-1}$ relative to the specific glucose uptake rate. Arrowheads indicate the primary direction of the determined fluxes. Arrows in the grey indicate the withdrawal of the precursors for biosynthesis. Abbreviations: G6P, glucose-6-phosphate; F6P, fructose-6-phosphate; T3P, triose-3-phosphate; PEP, phosphoenolpyruvate; PYR, pyruvate; 6PG, 6-phosphogluconate; Ru5P, ribulose-5-phosphate; X5P, xylulose-5-phosphate; R5P, ribose-5-phosphate; Sed7P, sedoheptulose-7-phosphate; AcCoA, acetyl-CoA; Ace, acetate; OAA, oxaloacetate; IsoCit, isocitrate; 2-KG, 2-ketoglutarate; Suc, succinate; Fum, fumarate; Mal, malate; E4P, erythrose-4-phosphate.

present enzyme activity assay, and the Ppc reaction remained to examine whether its flux was zero in the mutant. Therefore, the resulting network consisted of 23 reactions with 20 metabolites, generating a stoichiometric matrix with a rank of 20 (see Appendix B). The fluxes of Pgi, Pyk, CS were chosen as the net free fluxes, and 11 exchange fluxes (Pgi, Eno, Rpi, Rpe, Tkt1, Tkt2, Tal, ICDH, Fum, Mdh, Ppc/Pck) were considered. In both cases, the free fluxes were obtained by minimizing the error criterion originating from the weighted residuals of the metabolite balances as well as the weighted residuals between the estimated and the measured GC–

MS and 2D NMR signals [15]. The modified minimization algorithm [16] was used to compute the intracellular fluxes. A set of intracellular fluxes was then determined as the best fit to the experimentally determined data using a parameter fitting approach.

3. Results

3.1. Growth characteristics of the *ppc* mutant *E. coli*

The aerobic batch cultures of both the *ppc* mutant and the parental strain were repeated three times using glucose as a carbon source. Growth parameters at the exponential growth phase are shown in Table 1. The *ppc* mutant grew more slowly at a lower glucose consumption rate compared to the wild type. The carbon dioxide evolution rate was also reduced in the *ppc* mutant. More interestingly, little acetate was excreted in the *ppc* mutant during the whole period of the cultivation, whereas the wild type *E. coli* produced acetate significantly. As a consequence, an improvement of biomass yield on glucose was observed in the *ppc* mutant.

3.2. Enzyme activity changes in response to *ppc* mutation

Some key enzyme activities of central metabolism were assayed for the cells grown at the exponential growth phase (Table 2). Ppc activity was not detected in the *ppc* mutant, which confirmed the *ppc* knockout. In contrast, the wild type *E. coli* showed high Ppc activity, indicating that this anaplerotic pathway plays an important role in metabolism. The activity of PEP carboxykinase (Pck), which catalyzes the reverse reaction to Ppc, was also considerably lower in the *ppc* mutant (0.05-fold). The activities of the glycolytic enzymes such as hexokinase (Hex), glucose phosphate isomerase (Pgi), phosphofructose kinase (Pfk), fructose biphosphate aldolase (Fba) and glyceraldehyde-3-phosphate dehydrogenase (GAPDH) and the pentose phosphate

Table 1

Exponential growth parameters of the wild type *E. coli* and its *ppc* mutant grown on glucose under aerobic condition

Parameter	Wild type	<i>ppc</i> mutant
μ_{max} (h^{-1})	0.41	0.34
q_{glc} ($\text{mmol g}^{-1} \text{ h}^{-1}$) ^a	5.61	3.16
q_{CO_2} ($\text{mmol g}^{-1} \text{ h}^{-1}$) ^b	3.38	2.47
Q_{acc} (mmol g^{-1}) ^c	0.22	0.00
$Y_{\text{biomass}/\text{glc}}$ (g g^{-1}) ^d	0.48	0.55

Results represent the mean values of three independent experiments.

^a Specific glucose consumption rate.

^b Specific carbon dioxide evolution rate.

^c Specific acetate production rate.

^d Yield of biomass on glucose.

Table 2
Specific enzyme activities of the wild type *E. coli* and its *ppc* mutant grown on glucose under aerobic condition

Enzyme	Wild type	<i>ppc</i> mutant
Hexokinase (Hex)	0.0752 ± 0.0001	0.0466 ± 0.0001
Glucose phosphate isomerase (Pgi)	2.078 ± 0.004	0.436 ± 0.002
Phosphofructose kinase (Pfk)	0.564 ± 0.003	0.170 ± 0.002
Fructose biphosphate aldolase (Fba)	0.675 ± 0.003	0.0607 ± 0.0005
Glyceraldehyde-3-phosphate dehydrogenase (GAPDH)	0.692 ± 0.004	0.0899 ± 0.0005
Pyruvate kinase (Pyk)	0.220 ± 0.005	0.534 ± 0.004
Phosphoenolpyruvate carboxylase (Ppc)	0.0448 ± 0.0005	n.d. ^a
Phosphoenolpyruvate carboxykinase (Pck)	0.0427 ± 0.0004	0.0021 ± 0.0004
NADP ⁺ -specific malic enzyme (Mae)	0.067 ± 0.002	0.082 ± 0.002
NAD ⁺ -specific malic enzyme (Sfc)	0.088 ± 0.005	n.d.
Glucose-6-phosphate dehydrogenase (G6PDH)	0.245 ± 0.002	0.170 ± 0.002
6-Phosphogluconate dehydrogenase (6PGDH)	0.426 ± 0.003	0.00085 ± 0.00004
Citrate synthase (CS)	0.319 ± 0.002	0.369 ± 0.003
Aconitase (Acn)	0.115 ± 0.002	0.179 ± 0.002
Isocitrate lyase (Icl)	0.0361 ± 0.0003	0.113 ± 0.004
Isocitrate dehydrogenase (ICDH)	2.230 ± 0.002	0.971 ± 0.004
Malate dehydrogenase (MDH)	0.121 ± 0.007	0.193 ± 0.006

Values are the averages with standard deviations from three independent measurements. The unit of the enzyme activity is $\mu\text{mol min}^{-1} \text{mg (protein)}^{-1}$. Overall E–D pathway activity is represented as $\text{mg (pyruvate) min}^{-1} \text{mg (protein)}^{-1}$.

^aNot detected.

pathway enzymes such as glucose-6-phosphate dehydrogenase (G6PDH), 6-phosphogluconate dehydrogenase (6PGDH) and tansaldolase (Tal) were all significantly decreased in the *ppc* mutant (Table 2). These data were well supported by the slower growth and lower glucose utilization of the *ppc* mutant *E. coli* (Table 1). However, Pyk (pyruvate kinase) was an exception in that it was increased 2.4-fold (Table 2). The upregulation of Pyk was expected to channel more carbon flux from PEP to pyruvate due to the blockage of Ppc in the *ppc* mutant. Accordingly, CS, the first enzyme of the TCA cycle, was upregulated 1.8-fold in the *ppc* mutant (Table 2). This upregulation was expected to increase the carbon flux from pyruvate into the TCA cycle for the replenishment of OAA in response to the Ppc defect. The activities of aconitase (Acn) and malate dehydrogenase (MDH), but not isocitrate dehydrogenase (ICDH), in the TCA cycle increased in a coordinate manner. It is reported that CS and Acn, but not ICDH, are regulated coordinately, which might be due to the fact that citrate is an activator of Acn [17]. More interestingly, isocitrate lyase (Icl), encoded by *aceA* involved in the glyoxylate shunt was significantly induced by about 3.1-fold in the *ppc* mutant (Table 2). This regulation pattern clearly demonstrates that the *E. coli ppc* mutant utilized an alternative anaplerotic pathway, the glyoxylate shunt, to replenish OAA in response to the blockage through Ppc.

3.3. Variation of intracellular metabolite levels in the *ppc* mutant

The concentrations of some key intracellular metabolites were measured and the results were shown in

Table 3
Intracellular metabolite concentrations in the wild type *E. coli* and its *ppc* mutant grown on glucose under aerobic condition

Intracellular metabolite (mM)	Wild type	<i>ppc</i> mutant
G6P	0.68 ± 0.09	1.213 ± 0.13
F6P	0.29 ± 0.06	0.48 ± 0.07
F1,6P	1.01 ± 0.1	3.1 ± 0.21
PEP	0.07 ± 0.006	0.2 ± 0.06
6PG	0.38 ± 0.07	0.56 ± 0.09
AcCoA	0.13 ± 0.04	0.077 ± 0.005
OAA	0.03 ± 0.001	n.d. ^a

Values are the averages with standard deviations from three independent measurements. Cell volume: $2.55 \mu\text{g (DCW)}^{-1}$.

^aNot detected.

Table 3. The glycolytic intermediates such as G6P, F6P, F1,6P and PEP and the pentose phosphate pathway intermediate such as 6PG accumulated in the *ppc* mutant due to the inhibition of enzyme activities in their related pathways. In contrast, the intracellular concentration of AcCoA decreased in the *ppc* mutant, implying the higher activity of the TCA cycle relative to glycolysis. OAA could not be detected in the *ppc* mutant due to its low abundance, but it was detected in the wild type at a low concentration, implying that the intracellular OAA was limiting in the *ppc* mutant.

3.4. Changes in metabolic flux distributions in response to *ppc* mutation

Figs. 1 and 2 show the intracellular flux distributions in the wild type *E. coli* and its *ppc* mutant. Three notable differences between the wild type and its *ppc* mutant can be observed. First, 50.7% of carbon flux was channeled through Ppc in the wild type, and the backflow through

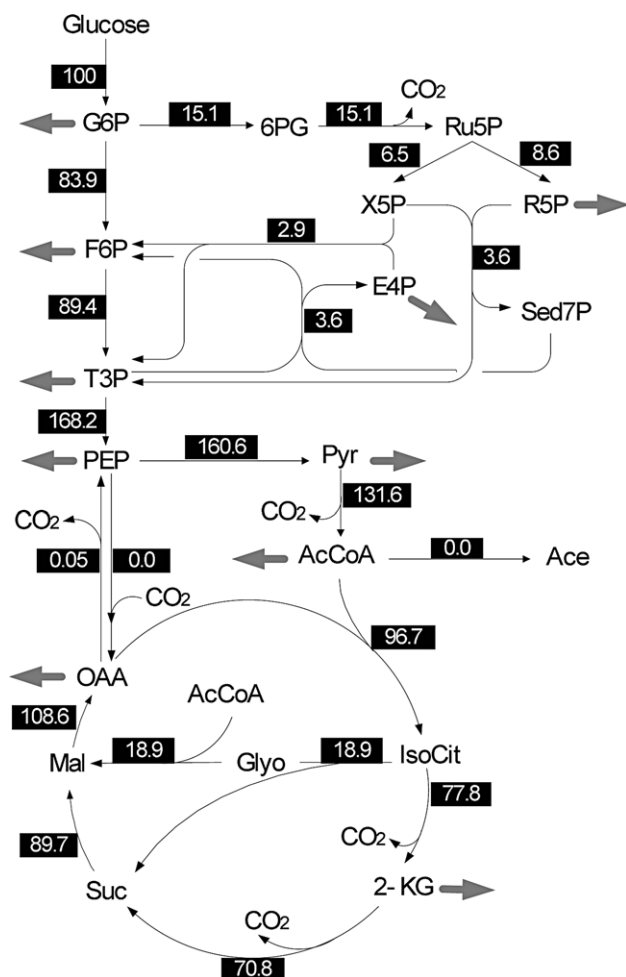


Fig. 2. Metabolic flux distribution in the chemostat culture of the *ppc* mutant *E. coli*. Numbers in the black box represent the estimated net fluxes at a dilution rate of 0.2 h^{-1} . Abbreviations: Glyo, glyoxylate. Consult the legend to Fig. 1 for details.

Pck was also high, accounting for 23.6% of the total glucose consumed. As predicted, there was no flux through Ppc in the *ppc* mutant. Moreover, the flux from OAA to PEP catalyzed by Pck was also significantly

decreased to only 0.05% in the *ppc* mutant. These flux results are in consistency with those of the enzyme activities (Table 2), which was also indicated by the visual observation of the ^{13}C - ^{13}C scalar coupling multiplet patterns of asp2 and phe2 (Table 4). The da and dd components in the multiplets of asp2 relate to the intact C2–C3 connectivity of the OAA molecule (the precursor of asp). Since the intact C2–C3 fragments of OAA can be introduced only by the anaplerotic reaction of Ppc, the absence of da and dd components of asp2 in the *ppc* mutant reflected the lack of in vivo activity of Ppc. In addition, the lower abundance of db component in phe2 in the *ppc* mutant implied less intact C1–C2 fragments of PEP molecule due to the low activity of Pck. Second, the glyoxylate shunt channeled 18.9% of the carbon flux in the *ppc* mutant. Visual inspection of the ^{13}C - ^{13}C multiplets of asp2 revealed a higher abundance of the db component in the *ppc* mutant (Table 4), which reflected the contribution of the glyoxylate shunt in excessive intact C1–C2 and C3–C4 connectivities [10,18]. Upregulation of Icl activity in the *ppc* mutant (Table 2) supported the consistency with this flux analysis result. The remaining carbon flux through ICDH via the TCA cycle was still larger than that of the wild type, implying that more NADPH required for biosynthesis could be generated via the TCA cycle in the *ppc* mutant. Third, 26.8% of the carbon flux was channeled through the oxidative pentose phosphate pathway in the wild type *E. coli*, in contrast to only 15.1% in the *ppc* mutant.

4. Discussion

PEP is a critical metabolite in *E. coli*, not only because of its role in the PTS system as a phosphoryl donor, but also in the regulation of many enzymes as an effector. It accumulated in the *ppc* mutant and allosterically inhibited some of the glycolytic enzymes such as Pgi and Pfk [14]. Inhibition of these enzymes led to higher intracellular concentrations of their intermediates

Table 4

2D proton-detected heteronuclear ^1H , ^{13}C multiple-quantum correlated nuclear magnetic resonance (2D HMQC NMR) spectra of cellular amino acids in the wild type *E. coli* and its *ppc* mutant

Atom	Wild type				<i>ppc</i> mutant			
	s	da	db	dd	s	da	db	dd
ala2	0.10	0.12	0.06	0.71	0.08	0.09	0.05	0.78
ala3	0.42	0.58	–	–	0.25	0.75	–	–
asp2	0.48	0.14	0.29	0.08	0.43	0.00	0.57	0.00
glu4	0.38	0.01	0.54	0.07	0.28	0.01	0.65	0.06
gly2	0.37	0.63	–	–	0.23	0.77	–	–
ile2	0.50	0.01	0.37	0.11	0.39	0.07	0.49	0.04
ile6	0.44	0.56	–	–	0.29	0.71	–	–
phe2	0.16	0.16	0.10	0.58	0.13	0.10	0.02	0.75
thr3	0.47	0.49	–	0.04	0.37	0.57	–	0.06
thr4	0.55	0.45	–	–	0.59	0.41	–	–
val2	0.35	0.05	0.51	0.06	0.20	0.05	0.67	0.05

such as F6P and F1,6P, which in turn affected some other enzymes. For instance, the key glycolytic enzyme hexokinase, is thought to be allosterically inhibited by its product G6P [14]. G6PDH is allosterically inhibited by FDP and PRPP and induced by glucose, while 6PGDH is inhibited by FDP, PRPP, GAP, Ru5P, E4P and NADPH and induced by gluconate [19]. Apparently, the higher concentration of intracellular F1,6P in the *ppc* mutant partially caused the downregulation of both enzymes. In addition, the higher flux through the TCA cycle produced more NADPH in the *ppc* mutant, which may be also considered a reason for the downregulation of 6PGDH. The transcript of the glucose transport gene, *ptsG*, was also associated with the accumulation of the glycolytic intermediates such as G6P and F6P that degraded the mRNA of *ptsG* by activating RNaseP enzyme [20]. Both downregulation of the glycolytic and pentose phosphate pathway enzymes resulted in the slower growth rate and lower glucose uptake rate in the *ppc* mutant (Table 1). The remarkably reduced Pck activity in the *ppc* mutant was considered to be caused by the higher intracellular concentration of PEP since Pck is allosterically inhibited by nucleotides, ATP and PEP [21].

It is known that the supply of OAA from PEP either via Ppc or the glyoxylate shunt is required for biosynthesis in *E. coli*, and Ppc is the main route for glucose metabolism [14]. The present results demonstrated that *E. coli* activated an alternative anaplerotic pathway, the glyoxylate shunt, for the replenishment of OAA in response to *ppc* knockout. The regulation of the glyoxylate shunt in *E. coli* has been demonstrated to be the result of reversible phosphorylation of the isocitrate dehydrogenase [13,22]. The reversible phosphorylation/inactivation of ICDH is catalyzed by a bifunctional enzyme, ICDH kinase/phosphatase. A variety of intracellular effectors affect ICDH kinase/phosphatase including OAA that inhibits ICDH kinase and stimulates the phosphatase [23]. The present result showed that the intracellular OAA concentration decreased in the *ppc* mutant (Table 3), which might have caused the phosphorylation of ICDH. The activation of the glyoxylate shunt contributed to the reduction in carbon dioxide production in the *ppc* mutant.

Acknowledgements

This research was supported in part by a grant from New Energy and Industrial Technology Development Organization (NEDO) of the Ministry of Economy, Trade and Industry of Japan (Development of Technological Infrastructure for Industrial Bioprocess Project). We are grateful to Drs. T. Baba and H. Mori, Keio University, for providing the bacterial strains.

Appendix A. Metabolic reactions for the wild type *E. coli*

Enzymes	Reactions	Coding genes
Hex	glucose+PEP → G6P+Pyr	<i>glk</i>
Pgi	G6P ↔ F6P	<i>pgi</i>
Fba	F6PT3P+T3P	<i>fba</i>
Eno	T3P ↔ PEP	<i>eno</i>
Pyk	PEP → Pyr	<i>pyk</i>
G6PDH	G6P → 6PG	<i>zwf</i>
6PGDH	6PG → Ru5P+CO ₂	<i>gnd</i>
Rpi	Ru5P ↔ R5P	<i>rpi</i>
Rpe	Ru5P ↔ X5P	<i>rpe</i>
Tkt1	R5P+X5P ↔ Sed7P+T3P	<i>tkt1</i>
Tkt2	E4P+X5P ↔ F6P+T3P	<i>tkt2</i>
Tal	S7P+T3P ↔ F6P+E4P	<i>tal</i>
PDHc	Pyr → AcCoA+CO ₂	<i>aceEF, lpdA</i>
CS	AcCoA+OAA → IsoCit	<i>gltA</i>
ICDH	IsoCit ↔ 2-KG+CO ₂	<i>icd A</i>
2-KGDH	2-KG → Suc+CO ₂	<i>sucAB, lpdA</i>
Fum	Suc ↔ Mal	<i>fum</i>
Mdh	Mal ↔ OAA	<i>mdh</i>
Ppc/Pck	PEP+CO ₂ ↔ OAA	<i>ppc/pck</i>
Mez	Mal → Pyr+CO ₂	<i>mez</i>
Ack	AcCoA → Ace	<i>ackA</i>

Appendix B. Metabolic reactions for the *ppc* mutant *E. coli*

Enzymes	Reactions	Coding genes
Hex	glucose+PEP → G6P+Pyr	<i>glk</i>
Pgi	G6P ↔ F6P	<i>pgi</i>
Fba	F6P → T3P+T3P	<i>fba</i>
Eno	T3P ↔ PEP	<i>eno</i>
Pyk	PEP → Pyr	<i>pyk</i>
G6PDH	G6P → 6PG	<i>zwf</i>
6PGDH	6PG → Ru5P+CO ₂	<i>gnd</i>
Rpi	Ru5P ↔ R5P	<i>rpi</i>
Rpe	Ru5P ↔ X5P	<i>rpe</i>
Tkt1	R5P+X5P ↔ Sed7P+T3P	<i>tkt1</i>
Tkt2	E4P+X5P ↔ F6P+T3P	<i>tkt2</i>
Tal	S7P+T3P ↔ F6P+E4P	<i>tal</i>
PDHc	Pyr → AcCoA+CO ₂	<i>aceEF, lpdA</i>
CS	AcCoA+OAA → IsoCit	<i>gltA</i>
ICDH	IsoCit ↔ 2-KG+CO ₂	<i>icd A</i>
2-KGDH	2-KG → Suc+CO ₂	<i>sucAB, lpdA</i>
Fum	Suc ↔ Mal	<i>fum</i>
Mdh	Mal ↔ OAA	<i>mdh</i>
Icl	IsoCit → Glyo+Suc	<i>aceA</i>
MS	Glyo+AcCoA → Mal	<i>aceB</i>
Ppc/Pck	PEP+CO ₂ ↔ OAA	<i>ppc/pck</i>
Mez	Mal → Pyr+CO ₂	<i>mez</i>
Ack	AcCoA → Ace	<i>ack A</i>

References

- [1] Flores, S., Gosset, G., Flores, N., de Graaf, A.A. and Bolivar, F. (2002) Analysis of carbon metabolism in *Escherichia coli* strains with an inactive phosphotransferase system by ^{13}C labeling and NMR spectroscopy. *Metab. Eng.* 4, 124–137.
- [2] Sauer, U., Lasko, R.W., Fiaux, J., Hochuli, M., Glaser, R., Szyperski, T., Wuthrich, K. and Bailey, J.E. (1999) Metabolic flux ratio analysis of genetic and environmental modulations of *Escherichia coli* central carbon metabolism. *J. Bacteriol.* 181, 6679–6688.
- [3] Chang, D., Jung, H., Rhee, J. and Pan, J. (1999) Homofermentative production of D-lactate or L-lactate in metabolically engineered *Escherichia coli* RR1. *Appl. Environ. Microbiol.* 65, 1384–1389.
- [4] Farmer, W.R. and Liao, J.C. (1997) Reduction of aerobic production by *Escherichia coli*. *Appl. Environ. Microbiol.* 63, 3205–3210.
- [5] Datsenko, K.A. and Wanner, B.L. (2000) One-step inactivation of chromosomal genes in *Escherichia coli* K12 using PCR products. *Proc. Natl. Acad. Sci. USA* 97, 6640–6645.
- [6] Zhao, J. and Shimizu, K. (2002) Metabolic flux analysis of *Escherichia coli* K12 using GC–MS and powerful flux calculation method. *J. Biotechnol.* 101, 101–117.
- [7] Peng, L. and Shimizu, K. (2003) Global metabolic regulation analysis for *Escherichia coli* K12 based on protein expression by 2-dimensional electrophoresis and enzyme activity measurement. *Appl. Microbiol. Biotechnol.* 61, 163–178.
- [8] Schaefer, U., Boos, W., Takors, R. and Weuster-Botz, D. (1999) Automated sampling device for monitoring intracellular metabolite dynamics. *Anal. Biochem.* 270, 88–96.
- [9] Bergmeyer, H.U. (1984) *Methods of Enzymatic Analysis*, 3rd edn, Vol. VI. *Metabolites I: Carbohydrates*, pp. 220–227. VCH, Weinheim, Germany.
- [10] Yang, C., Hua, Q., Baba, T., Mori, H. and Shimizu, K. (2003) Analysis of *Escherichia coli* anaerobic metabolism and its regulation mechanism from the metabolic response to altered dilution rates and phosphoenolpyruvate carboxykinase knockout. *Biotechnol. Bioeng.* 84, 129–144.
- [11] Schmidt, K., Nielsen, J. and Villadsen, J. (1999) Quantitative analysis of metabolic fluxes in *Escherichia coli* using two-dimensional NMR spectroscopy and complete isotopomer models. *J. Biotechnol.* 71, 175–190.
- [12] Paul Lee, W.N. (1991) Mass isotopomer analysis: theoretical and practical consideration. *Biol. Mass Spectrom.* 20, 451–458.
- [13] Cronan, J.J.E. and Laporte, D. (1999) Tricarboxylic acid cycle and glyoxylate bypass. In: *Escherichia coli and Salmonella: Cellular and Molecular Biology* (Neidhardt, F., Ed.). AMS, Mira Digital Publishing, Washington DC.
- [14] Fraenkel, D.G. (1999) Glycolysis. In: *Escherichia coli and Salmonella: Cellular and Molecular Biology* (Neidhardt, F., Ed.). AMS, Mira Digital Publishing, Washington DC.
- [15] Dauner, M., Bailey, J. and Sauer, U. (2001) Metabolic flux analysis with a comprehensive isotopomer model in *Bacillus subtilis*. *Biotechnol. Bioeng.* 76, 132–143.
- [16] Araúz-Bravo, M.J. and Shimizu, K. (2003) An Improved Method for Statistical Analysis of Metabolic Flux Analysis using Isotopomer Mapping Matrices with Analytical Expressions. *J. Biotechnol.* 105, 117–133.
- [17] Nakano, M.M., Zuber, P. and Sonenshein, A. (1998) Anaerobic regulation of *Bacillus subtilis* krebs cycle genes. *J. Bacteriol.* 180, 3304–3311.
- [18] Maaheimo, H., Fiaux, J., Cakar, Z.P., Bailey, J.E., Sauer, U. and Szyperski, T. (2001) Central carbon metabolism of *Saccharomyces cerevisiae* exposed by biosynthetic fractional of common amino acids. *Eur. J. Biochem.* 268, 2464–2479.
- [19] Sugimoto, S. and Shio, I. (1987) Regulation of 6-phosphogluconate dehydrogenase in *Brevibacterium flavum*. *Agric. Biol. Chem.* 51, 1257–1263.
- [20] Morita, T., Waleed, E., Yuya, T., Toshifumi, I. and Hiroji, A. (2003) Accumulation of glucose 6-phosphate or fructose 6-phosphate is responsible for destabilization of glucose transporter mRNA in *Escherichia coli*. *J. Biol. Chem.* 278, 15246–15608.
- [21] Krebs, A. and Bridger, W.A. (1980) The kinetic properties of phosphoenolpyruvate carboxykinase of *Escherichia coli*. *Can. J. Biochem.* 58, 309–318.
- [22] Cozzzone, A.J. (1998) Regulation of acetate metabolism by protein phosphorylation in enteric bacteria. *Annu. Rev. Microbiol.* 52, 127–164.
- [23] Holms, W.H. (1986) The central metabolic pathways in *Escherichia coli*: relationship between flux and control at a branchpoint, efficiency of conversion to biomass, and excretion of acetate. *Curr. Top. Cell. Regul.* 28, 69–105.